DOI: 10.18462/iir.gl2022.0084

# Thermodynamic analysis of a steam ejector chiller with ice storage

**Guglielmo VACCARO[(a)], Adriano MILAZZO*[(a)], Luca SOCCI[(a)], Lorenzo TALLURI[(a)]**

[(a)] Thermo Group - Department of Industrial Engineering – University of Florence, Florence, 50139, Italy
*Corresponding author: adriano.milazzo@unifi.it

## ABSTRACT

An integrated solar cooling and ice storage system for domestic air conditioning is presented. The system is based on an ejector that draws the water vapour directly from the ice storage and is designed to fulfil the cooling load requirements of a small building placed in central Italy. The presence of hot storage in the solar thermal subsystem and ice storage in the cooling cycle allows a peculiar working strategy that collects thermal energy in the daytime and produces the cooling effect at night. This improves the ejector efficiency, due to the limited condensing temperature achievable at night. The system operation has been simulated along the summer season and the required size of the hot and cold tanks and the solar collector's area have been calculated.

Keywords: Water, Heat powered refrigeration, Ejector, Ice storage, Solar cooling.

## 1. INTRODUCTION

Water is surely one of the best natural fluids for refrigeration, due to its low cost, absolute safety for operators and the environment, and high critical point. The use of water in vapour compression cycles, however, has been impaired by the high specific volume of steam at the evaporator exit and the high temperature at the end of compression. On the other hand, water is very successful as a refrigerant for heat-powered cycles, e.g., LiBr absorption chillers and steam ejector chillers. In these latter, steam is compressed in a dynamic device (the ejector) where the flow is supersonic, and hence huge volumetric flow rates may be accommodated in a relatively small space. The ejector has no moving parts and hence its cost, even if its volume is quite big, is tolerable. The cycle is powered by a heat source, possibly waste heat, or solar energy.

The use of solar energy is quite appealing for air conditioning, due to the proximity between the peak of cooling demand to the maximum availability of the energy source. An early example of a solar ejector cooling system was presented e.g. by Huang et al. (1998).

Due to phase shifts between air temperature and solar radiation or adverse weather conditions, cooling may be requested also when solar power is insufficient. In this case, a form of energy storage is requested. As pointed out by Chen et al. (2013), energy storage may be pursued on the hot as well on the cold side of the system. In the first case, hot storage is provided on the solar circuit, while in the second cold storage is present within the refrigeration system. This second option seems to be preferable.

In our view, the simplest and most promising proposal of solar ejector chiller with cold energy storage was made by Worall and Eames (2004). The cold storage relies on a natural substance, i.e. ice, as was done from the very early ages of refrigeration. Ice storage and steam refrigeration cycle are integrated within a single circuit. A detailed description and some experimental results from the proposed system were presented by Eames, Worall and Wu (2013). Our work starts from that scheme and adds some further analysis, applying the steam ejector chiller and the ice storage to an air conditioning system for a residential building located in Florence.

## 2. SYSTEM DESCRIPTION

The proposed system is schematically depicted in Fig. 1. A solar panel SP provides hot fluid that delivers thermal power to the hot storage HS. The steam flow rate produced within the generator, i.e. the tube coil

submerged in the HS, acts as motive (or “primary”) fluid within the ejector, reaching supersonic velocity through the convergent/divergent nozzle N. The motive flow entrains a “secondary” flow that comes from the suction port S of the ejector. This latter is placed directly on top of the evaporator E, which hosts the ice storage I.S. on its bottom. Primary and secondary flows mix within the ejector and recover pressure along with the diffuser D. Afterwards, the mixed flow returns to a liquid state in the condenser C. A bifurcation divides the liquid flow into two parts: the first goes back to the generator through a pump P; the second goes back to the evaporator, where it is sprayed onto the ice storage. There are three pressure levels: the lowest is found within the evaporator, the intermediate in the condenser, and the highest in the generator. Note the absence of an expansion valve on the liquid line between condenser and evaporator: the pressure drop is used to pulverize the liquid into small droplets, that should easily evaporate. Latent heat subtraction should cool down the remaining liquid, which is expected to form ice particles. The cooling load is applied by circulating a glycol-water mixture through a pipe that runs around the ice storage.

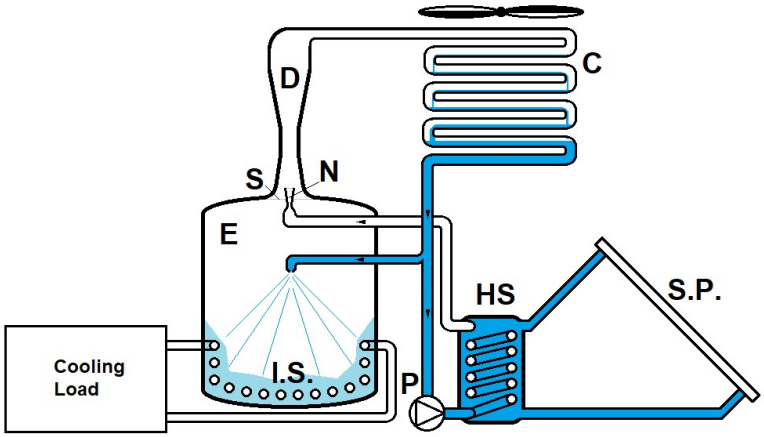


**Figure 1: Scheme of the proposed system**

According to the experience gained since 2013 on our prototype ejector chiller (Eames et al. 2013), we prefer a vertical layout with the condenser on top, which saves floor space and ensures a liquid head to the pump, avoiding cavitation problems. By the way, would the condenser be installed at a suitable height above the generator, water could be fed to the generator simply by gravity. This could be feasible e.g. in a building, placing the condenser on the roof and the generator in the basement. As pointed out in (Milazzo and Mazzelli 2017), the elimination of the pump is possible thanks to the high density of water in the liquid phase and relatively low saturation pressure at the generator. Without a pump, the system has no moving parts and the circuit would be completely sealed, avoiding any risk of air infiltration.

The proposed scheme is slightly different from the one presented by Eames, Worall and Wu (2013), where the liquid spray in the evaporator is produced by a pump that circulates the water collected on the bottom. In our view, extracting water with a pump from a low-pressure enclosure may pose cavitation problems. Therefore, we prefer to circulate the fluid that carries the cooling load at atmospheric pressure. In any case, the ejector operation, which is the most interesting and complex aspect of this project, is similar.

The ejector must be capable of extracting steam from the evaporator at the triple point pressure (612 Pa) and compressing it to the condenser pressure, which may be quite high if the condenser is air-cooled and placed in a Mediterranean climate. The generator receives hot fluid from the solar panel at temperatures that may range between 140 and 155°C. Obviously, the solar panels and the hot storage may be used also for sanitary water production or heating in the wintertime. Starting from these boundary conditions, we may try to evaluate a feasible performance for the proposed system.

### 2.1. Ejector modelling

The ejector is simulated through a thermodynamic model validated on the experimental results by Eames, Worall and Wu (2013). This gives a set of efficiency values for the various parts of the ejector, i.e. $\eta_{nozzle} = 0.98$ for the primary nozzle, $\eta_{mix} = 0.92$ for the mixing, and $\eta_{diff} = 0.97$ for the diffuser.

The relevant diameters along with the ejector are established for a given design point. The evaporator condition is fixed at the triple point of water. The generator design point is decided by the hot source temperature. The condenser temperature varies with the ambient temperature. Fluid properties are calculated via NIST Refprop 10 (https://www.nist.gov/srd/refprop).

An isentropic expansion is assumed in the convergent part of the motive nozzle, due to the very short length of this part. The nozzle throat is found imposing a maximum for the product $\rho v$ between density and velocity. In this way, we don't need to assume an ideal gas behaviour for the expanding vapour. The divergent part of the motive nozzle is calculated in two ways, depending on the working conditions:

a) If the generator temperature is higher than the design value the nozzle is under-expanded, i.e. the fluid pressure at the nozzle exit is higher than the suction pressure. In order to calculate the fluid state at the nozzle exit, a pressure value $P_{nozzle-out}$ is assumed. The ideal value of enthalpy at the nozzle exit is found as a function of $P_{nozzle-ou}$ and inlet entropy. From this value, given the nozzle efficiency, a real value can be calculated. The velocity at the nozzle outlet can be found from the enthalpy difference between inlet and outlet and from the mass flow rate divided by flow area and density. The calculation is iterated until convergence. Downstream of the nozzle, the fluid will reduce its pressure down to the suction value through a Prandtl-Meyer expansion. Assuming an efficiency $\eta_{exp} = 0.8$ for the Prandtl-Meyer expansion, the velocity at the end of the expansion may be found.

b) If the generator temperature is lower than the design value, the nozzle is over-expanded, i.e. the fluid pressure drops below the suction value. In this case, the nozzle efficiency will be reduced due to a normal shock in the divergent part of the nozzle or an oblique shock starting from the nozzle edge. Therefore, we must calculate a different value of efficiency. The pressure downstream of the shock must be equal to the suction pressure. A value for $\eta_{nozzle}$ is guessed and a value for the enthalpy at the nozzle exit is calculated. At this point, we may calculate two values of velocity and iterate on $\eta_{nozzle}$ until convergence.

A constant pressure mixing is assumed. An initial value may be guessed for the ejector entrainment ratio:

$$\omega = \frac{\dot{m}_{suction}}{\dot{m}_{motive}} \qquad \text{Eq. (1)}$$

The velocity of the mixed flow is calculated from the conservation of momentum, but the value is reduced by the mixing efficiency $\eta_{mix}$ to account for mixing losses. An energy balance along the mixing yields the total enthalpy of the mixed fluid. Therefore, the thermodynamic enthalpy may be used to calculate the density. Given the mixed flow rate, we may calculate the mixed flow area, which must be adjusted to the given value by changing the entrainment ratio until convergence is reached.

At this point, the mixed flow being supersonic, a normal shock occurs (actually a shock train develops in the middle part of the ejector, but this simplified view is commonly accepted in thermodynamic calculations). The conditions downstream of the shock are calculated imposing the conservation of momentum and mass flow rate. Enthalpy behind the shock may be calculated by imposing the conservation of total enthalpy. At this point, we may calculate a new density value as a function of pressure and enthalpy via NIST Refprop functions. The procedure is iterated until convergence. Refprop functions give also the entropy as a function of pressure and enthalpy.

Finally, the diffuser may be calculated imposing the conservation of total enthalpy and using the assumed efficiency of the diffuser. The calculated pressure at the exit may be compared with the one imposed by the condition at the condenser until convergence. The whole process is depicted in the flowchart in Figure 2. The simulated thermodynamic cycle is shown in Figure 3.

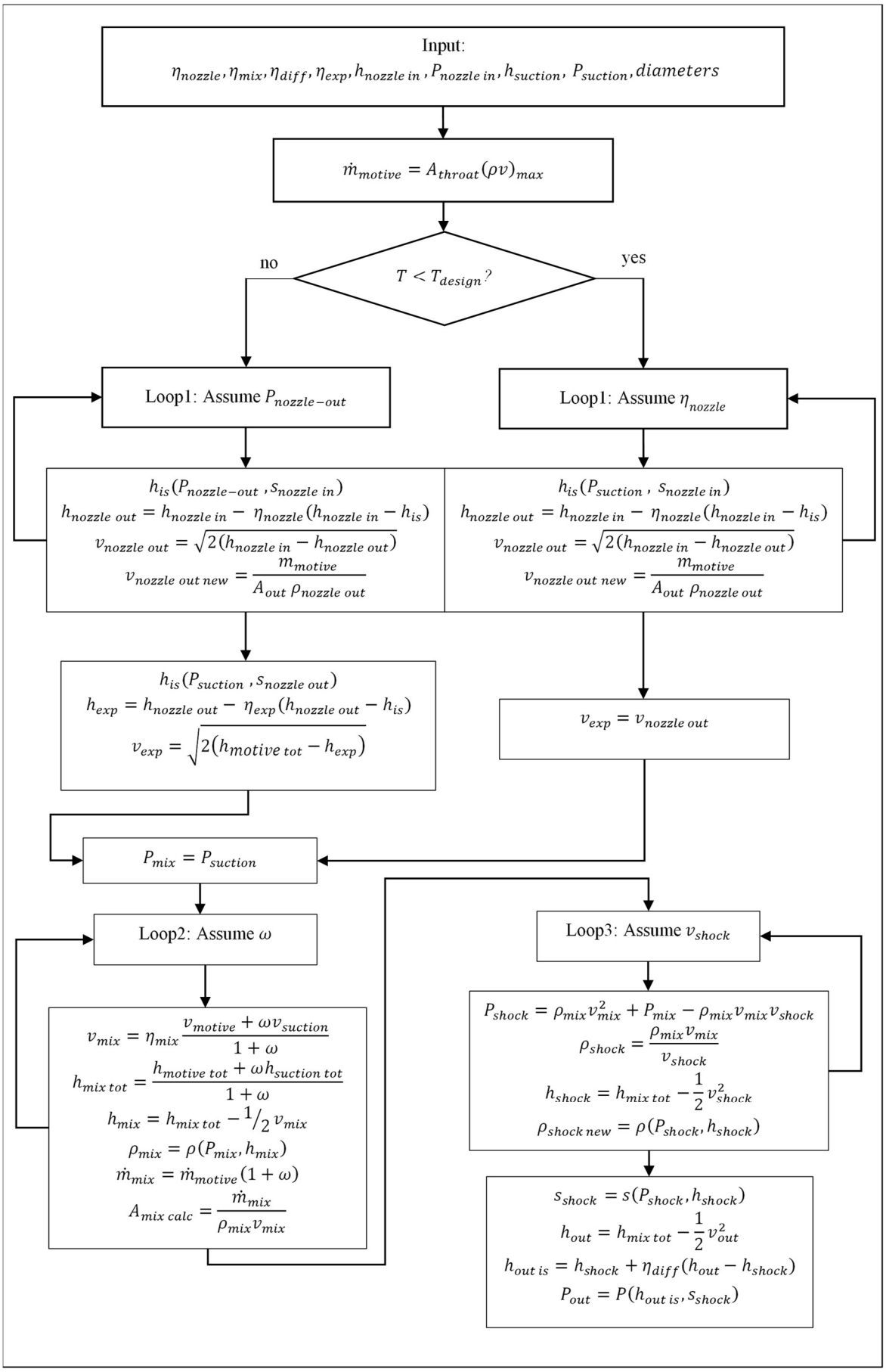


**Figure 2: Flow-chart of the ejector calculation**

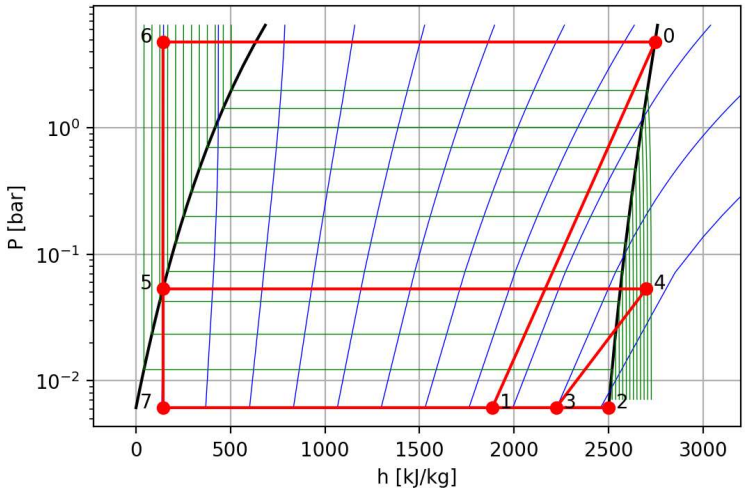


**Figure 3: Ph diagram of the thermodynamic cycle for $T_{hot}$ = 150°C and $T_{cond}$ = 34°C**

## 2.2. Calculation of the cooling demand

The cooling load to be met by the ejector cycle/thermal storage system was determined through a simulation of a reference building. The simulation was carried out using the software Design Builder, which implements the thermodynamic calculation code Energy Plus (https://energyplus.net).

The contributions to the heat balance can be summarised as follows: heat exchange through opaque surfaces (external walls and roof), heat exchange through transparent surfaces (glazed windows), internal generation due to household appliances and electronic devices, internal generation due to people, accidental air infiltration. Contributions to the thermal load deriving from controlled mechanical ventilation systems, which are rarely present in Italian residential buildings, have been excluded. The thermal transmittance of the opaque and transparent surfaces has been chosen according to the Italian legislative indications for the energy requalification of buildings, while the sources of internal heat generation have been evaluated from the indications of the ASHRAE 90.1 standard. External and internal convective heat transfer coefficients have been determined through the dynamic sub-hourly calculation performed by the software. The main features of the building are summarized in Table 1.

**Table 1. Reference building**

| **GEOMETRIC CHARACTERISTICS OF THE BUILDING** | | |
|---|---|---|
| Total volume | 630 | $m^3$ |
| Floor and roof area | 90 | $m^2$ |
| External opaque surfaces (walls and roofs) | 363 | $m^2$ |
| External transparent surfaces | 21 | $m^2$ |
| **THERMOPHYSICAL PROPERTIES OF OPAQUE SURFACES** | | |
| Thermal transmittance | 0.2 | $W/m^2/K$ |
| Infrared absorption-emission coefficient | 0.9 | |
| Solar radiation absorption coefficient | 0.7 | |
| **THERMOPHYSICAL PROPERTIES OF TRANSPARENT SURFACES** | | |
| Thermal transmittance (including frames) | 1.6 | $W/m^2/K$ |
| Solar radiation transmission coefficient | 0.6 | |
| **INTERNAL HEAT GENERATION** | | |
| Power density of household appliances, electronic devices | 15 | $W/m^2$ |
| Occupancy density | 0.05 | $People/m^2$ |
| Latent-total heat ratio for occupancy | 0.5 | |
| **VENTILATION FLOW RATES** | | |
| Incidental infiltration rate | 0.1 | Vol/h |

### 2.3. Solar thermal integration

Solar integration with the ejector chiller is brought through the combination of thermal panels and a water tank. Solar thermal collectors' energy output is strictly dependent on the local meteorological conditions. Knowing these for a chosen location, the desired size of the solar panel field can be determined. The sizing was done through a one-reference day model approach for a given location (https://energyplus.net).

A commercially available flat plate solar collector was considered for the solar thermal field [https://www.ferroli.com/media/ecotop%20vf-hf_ferroli_LOW_1.pdf]. Its efficiency ($\eta_0$) was modelled with a typical 2nd order Bliss-equation (Duffie and Beckman 2013). The efficiency of solar collectors ($\eta_0$) depends on incoming radiation (G), ambient temperature, and working fluid temperature increase.

$$\eta_{sc} = \eta_o - (a_1 + a_2 \Delta T)\frac{\Delta T}{G} \qquad \text{Eq. (2)}$$

The coefficients $\eta_o$, $a_1$ and $a_2$ are usually provided by the manufacturer of the collector. ΔT is the temperature difference between the average Heat Transfer Fluid (HTF) temperature and the ambient temperature. The HTF inlet and outlet temperatures are assumed as known at the design conditions.

The useful heat gain from the solar field is meant to warm up the water of the hot storage to a fixed temperature to be utilized during the chiller cycle operation.

The solar field surface A and, thus, the number of solar collectors, was found iteratively in a way that the daily solar heat yield was able to satisfy ejector chiller energy needs. The design assumptions for this section are presented in Table 2. Note that 22° is the typical slope for the roofs in Tuscany.

**Table 2. Solar thermal collector operating parameters**

| | |
|---|---|
| Location | Florence - 43.798, 11.253 |
| Slope of solar collector | 22° |
| Coefficients for Equation (2) | $\eta_0$= 0.623; $a_1$= 0.991; $a_2$=0.001 |

## 3. RESULTS

### 3.1. Ejector design

A first design of the ejector has been derived from the data reported in Eames, Worall and Wu (2013) in order to calibrate and validate the thermodynamic model. A good agreement has been reached between the experimental results and the calculated performance.

Then the system has been scaled to fulfil the request of the house described in section 2.2. Design conditions considered are: $T_{motive}$ = 150°C and $T_{cond}$ = 34°C. A velocity of 10 m/s was assumed for inlet and outlet velocity. The calculated dimensions for the ejector are resumed in Table 3.

**Table 3. Main dimensions of the ejector**

| | nozzle inlet | nozzle throat | nozzle exit | suction inlet | ejector throat | ejector outlet |
|---|---|---|---|---|---|---|
| Diameter (mm) | 20.83 | 3.97 | 36.18 | 313.85 | 50.49 | 211.47 |

From this design, the system performance has been calculated referring to typical summer conditions in Florence (Italy). When the saturation temperature of the motive flow is changed, the ejector performance changes as shown in Figure 4a. The motive flow rate increases with the motive pressure, while the entrained flow has a maximum at the design point. Consequently, the entrainment ratio (blue curve) is constantly

decreasing, but on the left of the design point, it has a lower slope than on the right. The slope change is due to the transition from under- to over-expanded nozzle operation.

This behaviour of supersonic ejectors is well known: for a fixed design, the entrainment ratio (and hence the COP of the ejector cooling system) decreases with the temperature of the heat source. However, the decrease of the motive flow reduces the capability of the ejector to overcome the exit pressure, i.e. its ability to cope with a high condensation temperature. This is clearly shown in Figure 4b, where the allowable condenser temperature steadily increases with the motive temperature, showing a slight change in the slope of the curves at the design point.

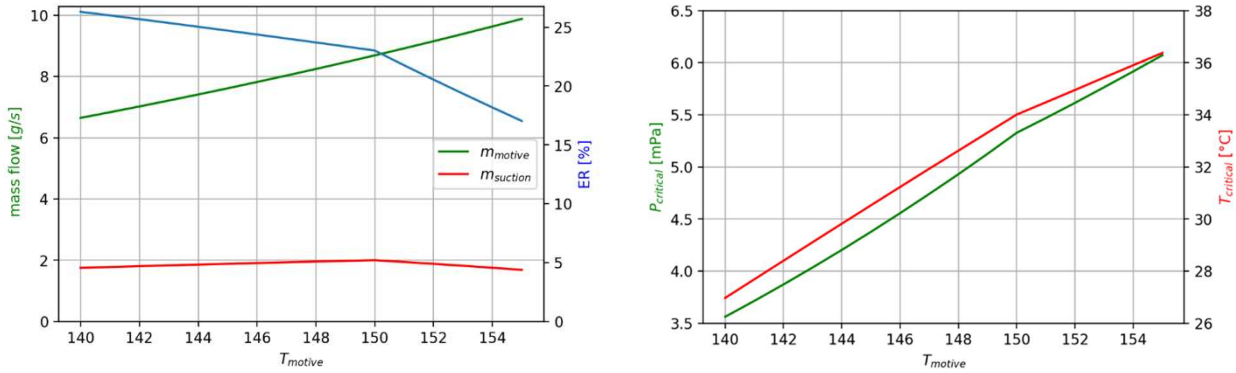


**Figure 4: a) Ejector performance as a function of motive temperature; b) Critical condenser pressure and temperature as a function of motive temperature**

Therefore, a compromise must be sought between the difficulty of reaching high temperatures with the solar panel and the possibility to operate the system on hot summer days. In order to satisfy these contrasting needs, we decided to operate the ejector at night, from 0:30 am to 6:30 am. This is possible thanks to the ice and hot storage tanks, that may transfer the cooling and the solar power from night to daytime.

Starting from the results of the ejector performance, a system simulation has been performed and the results are shown in Table 4. For each of the summer months, the table shows the cooling load, the maximum, minimum and average ambient temperature, the maximum night temperature, the hot source temperature.

**Table 4. System performance**

| | $Q_f$ | $T_{amb\text{-}max}$ | $T_{amb\text{-}min}$ | $T_{night\text{-}max}$ | $T_{hot}$ | $A_{coll\text{-}min}$ | Ice storage |
|---|---|---|---|---|---|---|---|
| | kWh | °C | °C | °C | °C | $m^2$ | kg |
| June | 19.1 | 35.3 | 20.9 | 23.1 | 148.6 | 30.2 | 24.2 |
| July | 18.7 | 37.1 | 22.5 | 24.7 | 151.5 | 33.9 | 23.8 |
| August | 15.8 | 37.5 | 23.5 | 25.6 | 153.4 | 33.7 | 20.1 |
| September | 8.73 | 33.0 | 19.5 | 21.5 | 146.4 | 15.4 | 11.1 |

The minimum area of the solar collectors is shown in the 7$^{th}$ column. The maximum value is needed in July (and is taken as the design value). On the other hand, the cold storage has a maximum in June, when the solar power is maximum and hence the system, as shown in the 2$^{nd}$ column, yields the maximum cooling power.

## 4. CONCLUSIONS

An integrated solar cooling and ice storage system for domestic air conditioning has been presented. The system was designed to evaluate the required heat and cooling load required by a small building placed in Florence. The results obtained demonstrate the feasibility of the system, with the proposed working strategy (loading the cooling tank at night). A pivotal point of the research has been the design of the ejector, which

allowed the proper dimensioning of the system, evaluating the optimal geometry and the required boundary conditions. The key results of the study may be summarized as follows:

- A solar cooling system that utilizes ice as the cold storage has been analysed and proved to be a possible solution for the satisfaction of the cooling load of a small building.
- The design temperature of the ejector has been determined to be around 150°C due to the condenser temperature which is 34°C.
- 4 representative days for months from June to September have been selected, allowing us to calculate the required size of the hot and cold tanks and the solar collector's area. The maximum required collectors' area is 34 $m^2$, the mass of the ice storage is 24.2 kg.

The cost and space requirements of the proposed system may hardly be competitive with a solar cooling system based on PV panels, batteries and a vapour compression cooling cycle. However, the proposed system can be manufactured with common, widely available materials, while systems based on electricity may pose problems of shortage for some basic components in the long term when "all-electric" systems will increase their market share. An LCA analysis would be required to highlight this aspect.

## NOMENCLATURE

| | | | |
|---|---|---|---|
| $\eta$ | efficiency | $s$ | entropy ($kJ \times kg^{-1} \times K^{-1}$) |
| $\rho$ | density ($kg \times m^{-3}$) | $T$ | temperature (K) |
| $\omega$ | entrainment ratio | **Subscripts** | |
| $v$ | velocity ($m \times s^{-1}$) | *exp* | expansion |
| $\dot{m}$ | mass flux ($kg \times s^{-1}$) | *is* | isentropic |
| $A$ | area ($m^2$) | *mix* | mixing |
| $h$ | enthalpy ($kJ \times kg^{-1}$) | *tot* | total |
| $P$ | pressure (Pa) | | |

## REFERENCES


Chen, X., Omer, S., Worall M., Riffat, S., 2013. Recent developments in ejector refrigeration technologies. Renewable and Sustainable Energy Reviews. 19, 629–651.

Duffie JA., Beckman WA., 2013, Solar Engineering of Thermal Processes, Fourth Edition, John Wiley & Sons Inc.

Eames, I.W., Milazzo, A., Paganini D., Livi M., 2013. The design, manufacture and testing of a jet-pump chiller for air conditioning and industrial application. Applied Thermal Engineering. 58, 234-240.

Eames, I.W. Worall, M., Wu, S., 2013. An experimental investigation into the integration of a jet-pump refrigeration cycle and a novel jet-spray thermal ice storage system. Applied Thermal Engineering. 53, 285-290

Huang, B.J., Chang, J.M., Petrenko W.A., Zhuk K.B., 1998. A solar ejector cooling system using refrigerant R141b. Solar Energy. 64(4-6),223-226.

Milazzo, A., Mazzelli, F., 2017. Future perspectives in ejector refrigeration. Applied Thermal Engineering. 121, 344-350

Worrall, M., Eames, I.W., 2004. An Experimental Investigation of a Jet-pump Thermal Ice Storage System Powered by Low-grade Heat; Proc. 3rd Int. Conference on Sustainable Energy Technologies, Nottingham, UK.